ACS Chemical Neuroscience

Research Article

pubs.acs.org/chemneuro

Magnetic Resonance Imaging of Mitochondrial Dysfunction and Metabolic Activity, Accompanied by Overproduction of Superoxide

Rumiana Bakalova,*[,†] Ekaterina Georgieva,[‡] Donika Ivanova,[‡] Zhivko Zhelev,[‡,§] Ichio Aoki,[†] and Tsuneo Saga[†]

[†]Molecular Imaging Center, National Institute of Radiological Science, 4-9-1 Anagawa, Inage-ku, Chiba 263-8555, Japan

[‡]Medical Faculty, Trakia University, 11 Armejska Str., Stara Zagora 6000, Bulgaria

[§]Institute of Biophysics & Biomedical Engineering, Bulgarian Academy of Sciences, 21 Acad. G. Bonchev Str., Sofia 1114, Bulgaria

Supporting Information

ABSTRACT: This study shows that a mitochondria-penetrating nitroxide probe (mito-TEMPO) allows detection of superoxide and visualization of mitochondrial dysfunction in living cells due to the effect of T_1 shortening in MRI. Mitochondrial dysfunction was induced by treatment of cells with rotenone and 2-methoxyestradiol (2-ME/Rot). The MRI measurements were performed on 7T MRI. The 2-ME/Rot-treated cells were characterized by overproduction of superoxide, which was confirmed by a conventional dihydroethidium test. In the presence of mito-TEMPO, the intensity of MRI signal in 2-ME/Rot-treated cells was ∼30−40% higher, in comparison with that in untreated cells or culture media. In model (cell-free) systems, we observed that superoxide, but not hydrogen peroxide, increased the intensity of T_1-weighted MRI signal of mito-TEMPO. Moreover, the superoxide restores the T_1-weighted MRI contrast of mito-TEMPOH, a noncontrast (diamagnetic) analogue of mito-TEMPO. This was also confirmed by using EPR spectroscopy. The results demonstrate that superoxide radical is involved in the enhancement of T_1-weighted MRI contrast in living cells, in the absence and presence of mito-TEMPO. This report gives a direction for discovering new opportunities for functional MRI, for detection of metabolic activity, accompanied by overproduction of superoxide, as well as by disturbance of the balance between superoxide and hydrogen peroxide, a very important approach to clarify the fine molecular mechanisms in the regulation of many pathologies. The visualization of mitochondrial activity in real-time can be crucial to clarify the molecular mechanism of the functional MRI in its commonly accepted definition, as a method for detection of neurovascular coupling.

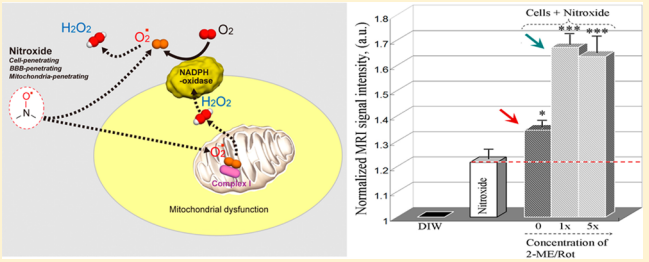

KEYWORDS: *Nitroxides, superoxide, hydrogen peroxide, magnetic resonance imaging, mitochondrial dysfunction*

Mitochondria play a central role in energy metabolism and apoptosis. In normal physiological conditions, electrons are derived from the mitochondrial electron-transport chain (ETC) during oxidative phosphorylation, and a proton-gradient is established across the inner mitochondrial membrane as an energy source for ATP synthesis.[1] This metabolic process is accompanied by production of reactive oxygen species (ROS) (mainly superoxide and hydrogen peroxide) within the ETC. Thus, the mitochondria are considered a major source of ROS in the cells. Normally, the superoxide can be converted into hydrogen peroxide by the superoxide dismutase (SOD). Thus, the level of intracellular superoxide is strongly regulated, which is important to maintain the redox-balance and cellular signaling.

In mitochondrial dysfunction, provoked by genetic mutations or xenobiotics (drugs), the electrons can escape from the ETC (especially at complex-I or complex-III), and they may react with molecular oxygen to form superoxide radicals inside or outside the mitochondria.[2,3]

The interference in both processes simultaneously, stimulation of superoxide generation via impairment of mitochondrial ETC and suppression of its elimination by SOD, will cause a severe accumulation of superoxide radicals, as well as other ROS, in the cells and development of redox imbalance.

This mechanism is widely discussed as a trigger of mitochondrial metabolic diseases, for example, neurodegenerative disorders and cancer.[4,5] These pathologies are associated with mitochondrial dysfunction and overproduction of ROS, which have completely opposite consequences for the cells. In cancer, the mitochondrial dysfunction provokes cell proliferation and immortalization, while during neurodegeneration it leads to loss of the affected neurons.[6−9]

It is widely accepted that the primary endogenous triggers of redox imbalance in cancer cells are (i) defective mitochondria (which are characterized by mutations in complex-I in the

Received: June 13, 2015
Accepted: September 14, 2015
Published: September 14, 2015

DOI: 10.1021/acschemneuro.5b00220
ACS Chem. Neurosci. 2015, 6, 1922−1929

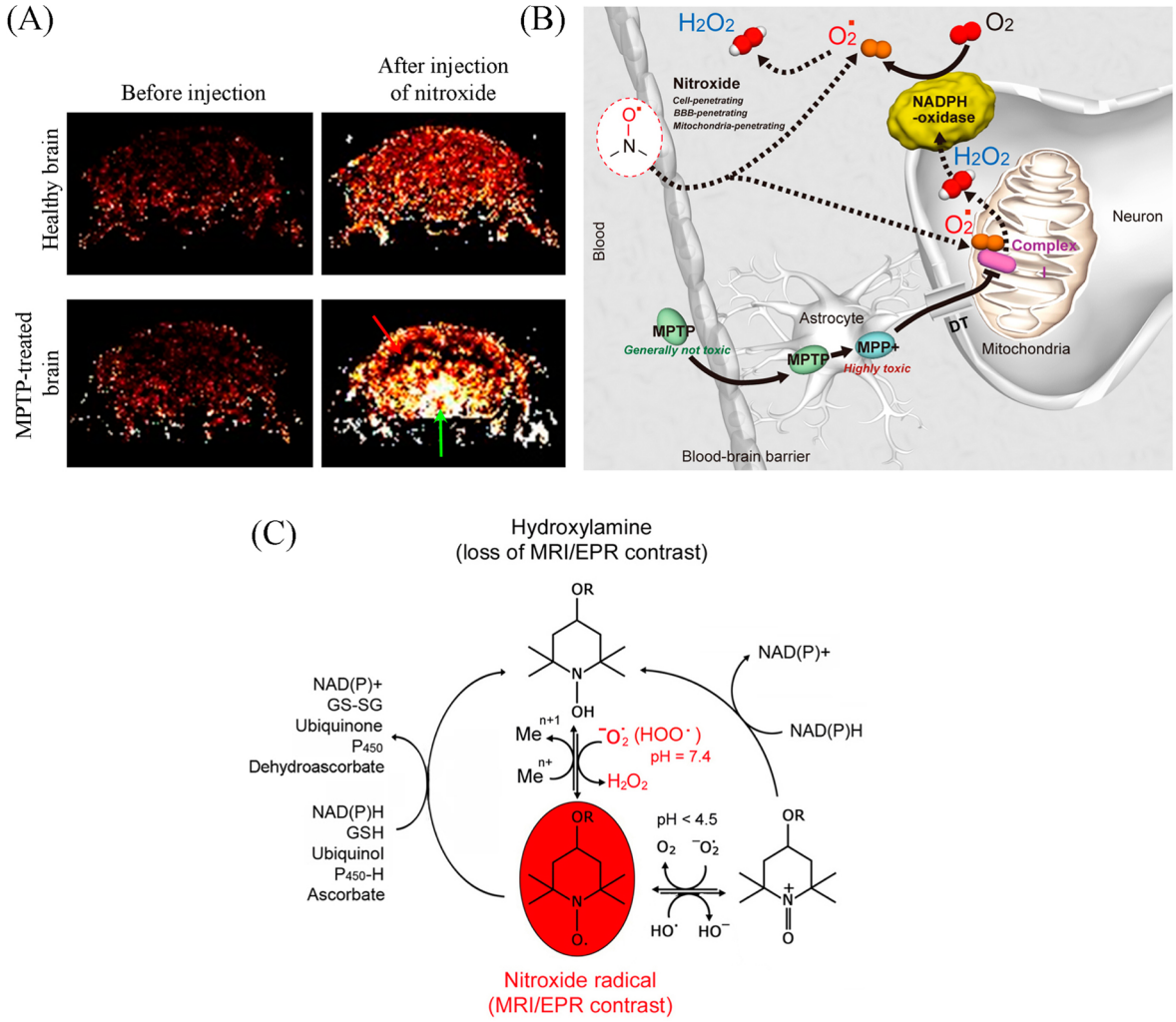

Figure 1. (A) MR imaging of tissue redox status in dopamine neurons [according to Zhelev et al.[17]]. Extracted nitroxide-enhanced MRI signal in the brain of healthy and MPTP-treated mice, obtained 5 min after injection of nitroxide (mito-TEMPO) (T_1-weighted MRI, gradient-echo). (B) Molecular hypothesis for enhancement of MRI signal in MPTP-affected and oxidatively active dopaminergic neurons [according to Vila and Przedborski[13] and Zhelev et al.[17]]. (C) Relationship between redox cycle and MRI/EPR contrast of the nitroxide probe [according to Bakalova et al.[15]]. Abbreviations: $O_2^{\bullet}$, superoxide radical; $HOO^{\bullet}$, protonated form of superoxide radical; H_2O_2, hydrogen peroxide; $HO^{\bullet}$, hydroxyl radical; DT, dopamine transporter; MPP+, 1-methyl-4-phenylpyridinium; MPTP, 1-methyl-4-phenyl-1,2,3,6-tetrahydropyridine; Me^{n+}/Me^{n+1}, transition metal ions; GSH/GS-SG, glutathione in reduced/oxidized form; P_{450}/P_{450}-H, cytochrome P450 in oxidized/reduced form; MRI, magnetic resonance imaging; EPR, electron paramagnetic resonance.

majority of cases) and (ii) up-regulated NADPH-dependent oxidase complex (NOX). Both components induce overproduction of superoxide or hydrogen peroxide as an initial event.[1,10−12]

A similar principle was described for neurodegenerative disorders, for example, the MPTP-mouse model of Parkinson's disease (Figure 1B).[13] After systemic intravenous administration of MPTP (which is a generally nontoxic protoxin), it rapidly crosses the blood−brain barrier (BBB) and is metabolized to 1-methyl-4-phenyl-2,3-dihydropyrrolidine (MPDP+) by the monoamine oxidase B (MAO-B) in non-dopamine cells (astrocytes) and then, probably by spontaneous oxidation, to 1-methyl-4-phenylpyrrolidine (MPP+).[13,14] MPP+ is the active toxic compound with high affinity to dopamine transporters. Thus, MPP+ can be delivered in the dopamine neurons. MPP+ is concentrated within the mitochondria, where it inhibits complex-I of the electron transport chain and impairs mitochondrial respiration. The inhibition of complex-I impedes the flow of electrons in the mitochondrial electron transport chain, resulting in an increased production of ROS (predominantly superoxide radicals and hydrogen peroxide) by mitochondria and subsequent activation of NOX, which causes additional production of superoxide and hydrogen peroxide in dopaminergic tissues.

Recently, we have found that the redox status of cancerous tissue and dopaminergic tissues of mice with parkinsonism is completely different from that of healthy tissues, and this can be visualized and analyzed by nitroxide-enhanced magnetic resonance imaging (MRI) on experimental animal models (Figure 1A).[15−17] The most important findings in these studies are that (i) the intensity of nitroxide-enhanced MRI signal is very strong in dopaminergic areas of MPTP-treated brain but not in the cortex of the MPTP-treated brain or dopaminergic region of the healthy brain (Figure 1A)[17] and (ii) the intensity of nitroxide-enhanced MRI signal is very strong in cancerous tissue, while in noncancerous tissues it disappears quickly.[15,16]

We assume that the enhancement of MRI signal in neurodegenerative or cancer tissues is a result of abnormal

DOI: 10.1021/acschemneuro.5b00220
ACS Chem. Neurosci. 2015, 6, 1922−1929

production of superoxide, hydrogen peroxide, or both by defective mitochondria and NOX, which dominate over the protective capacity of the endogenous redox pairs and antioxidants.[15−17]

This assumption is based on the data in the literature about the coupling between the redox cycle of nitroxide derivatives and their contrast properties in cell-free systems (in vitro) or animal models (ex vivo),[18−23] which are indicative of low production or overproduction of superoxide (Figure 1C).

To verify the validity of this hypothesis, in the present study, we used an experimental approach and methodology for visualizing superoxide production (based on impaired mitochondrial activity), using nitroxide-enhanced MRI on cultured cells subjected to oxidative stress.

An appropriate cellular model for impairment of mitochondrial ETC, accompanied by overproduction of superoxide, has been described by Huang et al.[24] and Pelicano et al.[1] The authors have used rotenone (Rot), a known inhibitor of mitochondrial complex-I, in combination with SOD inhibitor 2-methoxyestradiol (2-ME) to test their effect on cellular superoxide levels, using flow cytometry. The rotenone stops the electron flow through complex-I and thus causes an increase in superoxide production in the mitochondrial matrix (Figure 1S, Supporting Information). The 2-ME is used to inhibit the elimination of superoxide via inhibition of the mitochondrial superoxide dismutase (especially SOD2 isoenzyme). This causes a further accumulation of superoxide in the cells and strongly minimizes the production of hydrogen peroxide. Although some authors do not agree with the concept of direct inhibition of SOD by 2-ME,[25] all publications show that treatment with 2-ME increases superoxide production in cancer cells, via SOD-mediated or non-SOD-mediated mechanism(s).[1,24−28]

We used this experimental strategy to cause overproduction of superoxide in living cells, as a result of inhibition of the mitochondrial respiration, and to clarify its effect on the dynamics of nitroxide-enhanced MRI signal in cell suspensions. Two cell lines of identical origin were chosen, leukemic lymphocyte Jurkat and K562 (isolated from patients with acute lymphoblastic leukemia or chronic myeloid leukemia, respectively).

RESULTS AND DISCUSSION

The production of superoxide in cells treated by 2-ME/Rot was analyzed and verified by conventional DHE test with spectrofluorimetric detection (Figure 2). The cells incubated with 1× 2-ME/Rot for 12 or 24 h were characterized by overproduction of superoxide, 4 times higher than the control (untreated cells). The superoxide level in the cells incubated with 2-ME or Rot only was the same as the control level after 12 h incubation and slightly higher (about 50%) than the control level after 24 h incubation. This test confirms the overproduction of superoxide in cells (Jurkat) treated with 1× 2-ME/Rot at the selected experimental protocol. Similar data were also obtained on leukemia cells K562; the fluorescent intensity was ∼3.5 times higher in 2-ME/Rot-treated cells than in untreated.

In a separate experiment, we investigated the level of superoxide in cell suspensions (Jurkat), treated with different concentrations of 2-ME/Rot (1×, 2×, 5×, 10×, and 20×) for a short time at room temperature or a long time in incubator. The aim was to select the most appropriate conditions for induction of oxidative stress in the cell suspension, which is

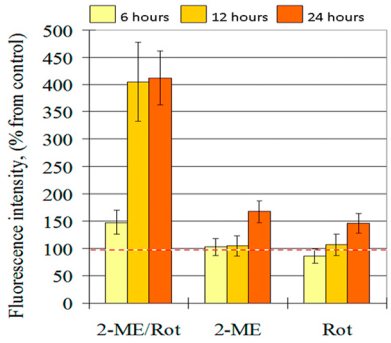

Figure 2. Level of superoxide in Jurkat cells treated with 2-methoxyestradiol (2-ME), rotenone (Rot) or their combination (2-ME/Rot) and analyzed with conventional dihydroethidium (DHE) test. Incubation conditions: Cells (3.5×10^6 cells/mL) were incubated for 6, 12, and 24 h with 300 nM 2-ME, 250 nM Rot, or both. Untreated cells were used as a control. Each cell suspension was analyzed as was described in Methods. The data were calculated as a percentage from control (untreated) cells. The fluorescence intensity of the DHE derivative in untreated cells was considered 100%. Mean + SD values from four independent experiments are shown in the graph.

characterized by a high level of superoxide and comparatively low cytotoxicity, for application in MRI experiments. The data are shown in Table 1S (see Supporting Information). The "acute treatment" of the cells with high concentrations of 2-ME/Rot (10× or 20×) for 30 min, as well as the "mild treatment" with lower concentrations of 2-ME/Rot (1×, 2×, or 5×) for 24 h lead to a significant increase of fluorescence intensity of DHE derivatives, accumulation of superoxide 3−4 times higher than in untreated cells without significant influence on cell viability (Table 2S, see Supporting Information). The long-term treatment of the cells with high concentrations of 2-ME/Rot (10× or 20×) induced cytotoxicity. Thus, in further MRI experiments on cells, we chose two protocols: "mild treatment" with 1× and 5× 2-ME/Rot for 24 h and "acute treatment" with 10× and 20× 2-ME/Rot for 30 min.

Figure 3 shows the dynamic of nitroxide-enhanced MRI signal in cell suspensions, before and 24 h after treatment with 2-ME/Rot at two different concentrations, 1× and 5×. In this case, 5× 2-ME/Rot suppressed proliferation (∼12−20%) but did not exhibit a significant cytotoxic effect within 24 h. Cell viability was ∼98−99% before the incubation and ∼94−96% after 24 h incubation. Treatment with 1× 2-ME/Rot did not cause any cytotoxic effect on Jurkat and K562 cells. Cells subjected to treatment with 2-ME/Rot (1× and 5×) for 24 h were characterized by a strong enhancement of T_1-weighted MRI contrast in the presence of mito-TEMPO. The intensity of nitroxide-enhanced MRI signal in 2-ME/Rot-treated cells was about 30−40% higher than that of mito-TEMPO in untreated cells or culture medium (Figure 3A2,B2, the green arrows versus the red dotted lines).

The nitroxide-enhanced MRI signal was ∼10% higher even in untreated leukemia cells, compared with the signal of mito-TEMPO in culture medium (Figure 3A2,B2, the red arrows versus the red dotted lines). It seems that the T_1 shortening effect of nitroxide is amplified in cancer cells. This fact could be very indicative about the mechanism(s) of T_1 shortening by nitroxide radical or superoxide radical in cell suspensions. The cancer cells (e.g., leukemic lymphocytes) are characterized by a high capacity for generation of superoxide or hydrogen peroxide due to their intrinsic mitochondrial dysfunction and

DOI: 10.1021/acschemneuro.5b00220
ACS Chem. Neurosci. 2015, 6, 1922−1929

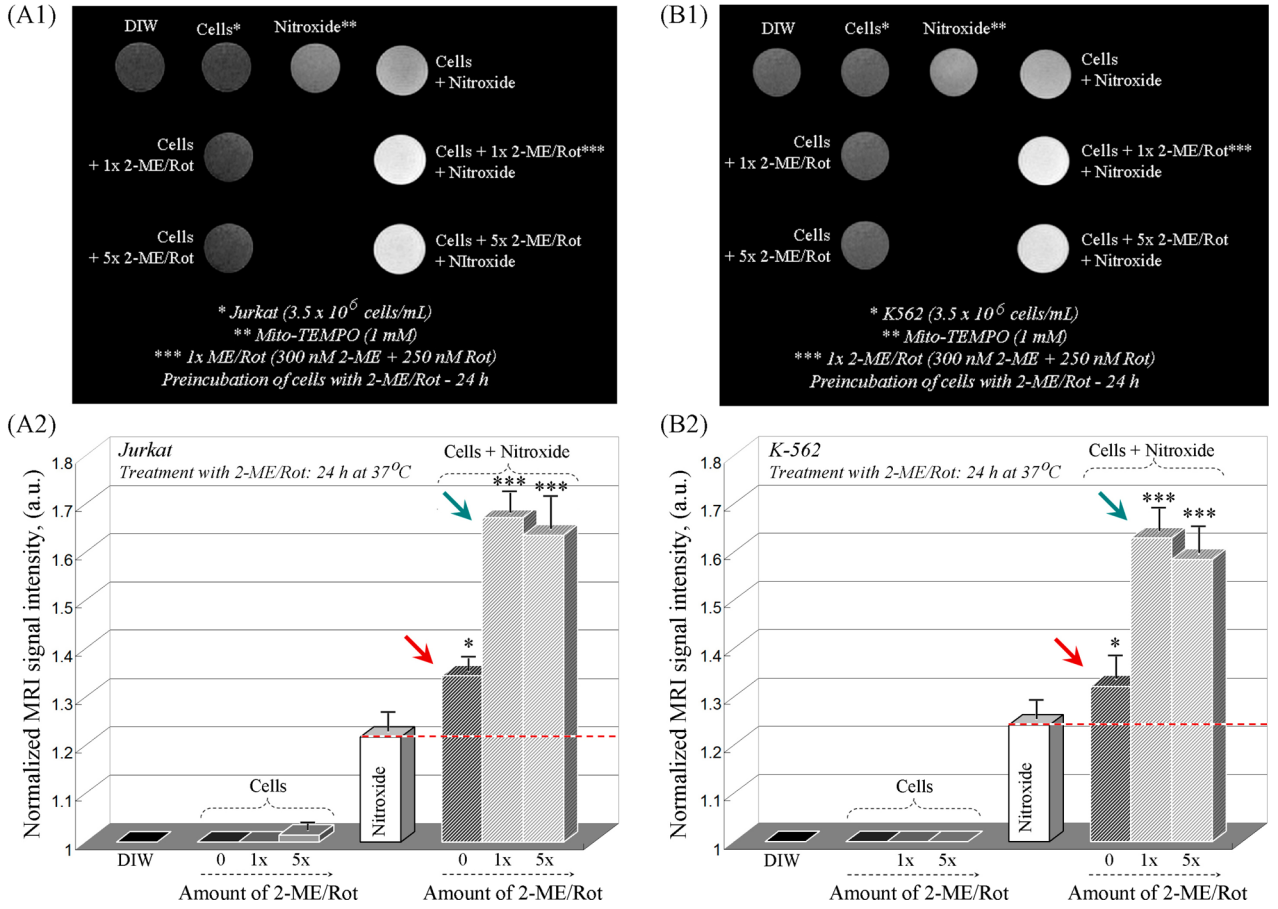

Figure 3. (A1, B1) Representative MR images of cell suspensions (A, Jurkat; B, K562) before and after treatment with 2-methoxyestradiol/rotenone (2-ME/Rot): Cells (3.5×10^6 cells/mL) were incubated for 24 h with 1× or 5× 2-ME/Rot (1× 2-ME/Rot = 300 nM 2-ME + 250 nM rotenone). Untreated cells were used as a control. Each cell suspension was separated in two MRI phantoms (in equal volumes), and mito-TEMPO (1 mM) was added to one of them. All samples were subjected to T_1-weighted MRI (spin−echo) ∼20 min after addition of mito-TEMPO. Other controls: DIW, deionized water; Nitroxide, 1 mM mito-TEMPO in culture medium. (A2, B2) Normalized intensity of the MRI signal of phantoms, described in panels A1 and B1. Mean + SD values from six independent experiments are shown in the graphs: $^*p < 0.05$; $^{**}p < 0.01$; $^{***}p < 0.001$ versus the MRI signal intensity of 1 mM mito-TEMPO in culture medium (the dotted red line).

up-regulation of NOX.[33] On the other hand, it is well-known that free radicals affect the relaxivity of protons, which results in T_1 shortening through a physical mechanism.[34] Therefore, the amplified signal (Figure 3A2,B2, the red arrows versus the red dotted lines) could be explained by interaction of superoxide with mito-TEMPO, which maintains the radical form of nitroxide in the cells, and its direct effect on proton relaxivity.

Figure 4 shows the dynamics of nitroxide-enhanced MRI signal in cell suspension, before and after acute treatment with 2-ME/Rot (10× and 20×) for 30 min. In this case, the viability of the 2-ME/Rot-treated cells was same as in untreated cells (∼98%). Cancer cells subjected to this acute treatment with high concentrations of 2-ME/Rot (10× and 20×) for 30 min were characterized by a strong enhancement of T_1-weighted MRI contrast in the presence of mito-TEMPO. The intensity of nitroxide-enhanced MRI signal in the 2-ME/Rot-treated cells was about 30−35% higher than that of mito-TEMPO in culture medium (Figure 4A2,B2, the green arrows versus the red dotted lines). In this experimental protocol, even in the absence of mito-TEMPO, the 2-ME/Rot-treated cells show a very slight T_1 shortening effect, especially Jurkat. Presumably, this is due to a higher baseline superoxide production in these cells, which could be detected using an acute treatment protocol. This protocol is also less time-consuming.

To clarify additionally the role of superoxide and hydrogen peroxide on the MRI signal, we performed MRI measurements in several chemical (cell-free) systems (see Figure 2S, Supporting Information): (i) deionized water containing nitroxide and potassium superoxide (which decays very quickly to superoxide radicals); (ii) deionized water containing nitroxide and hydrogen peroxide. The nitroxide probes were used in their contrast forms (which are radical and paramagnetic) or noncontrast analogues (which are reduced and diamagnetic): mito-TEMPO versus mito-TEMPOH; TEMPOL versus TEMPOH. It was observed that superoxide increased the MRI signal intensity of mito-TEMPO, while hydrogen peroxide (in physiologically relevant concentrations, below 1 mM) did not affect the MRI signal (Figure 2S, Supporting Information). Superoxide, but not hydrogen peroxide, recovers the T_1-weighted MRI contrast of mito-TEMPOH. Similar data were obtained using TEMPOL and its noncontrast analogue TEMPOH (Figures 3S and 4S, Supporting Information). These data confirmed the assumption that the T_1 shortening effect of nitroxide radical is amplified in the presence of superoxide, but not in the presence of hydrogen peroxide.

These observations were also confirmed by EPR spectroscopy on cell-free systems (Figure 5; Figures 5S−7S, Supporting

DOI: 10.1021/acschemneuro.5b00220
ACS Chem. Neurosci. 2015, 6, 1922−1929

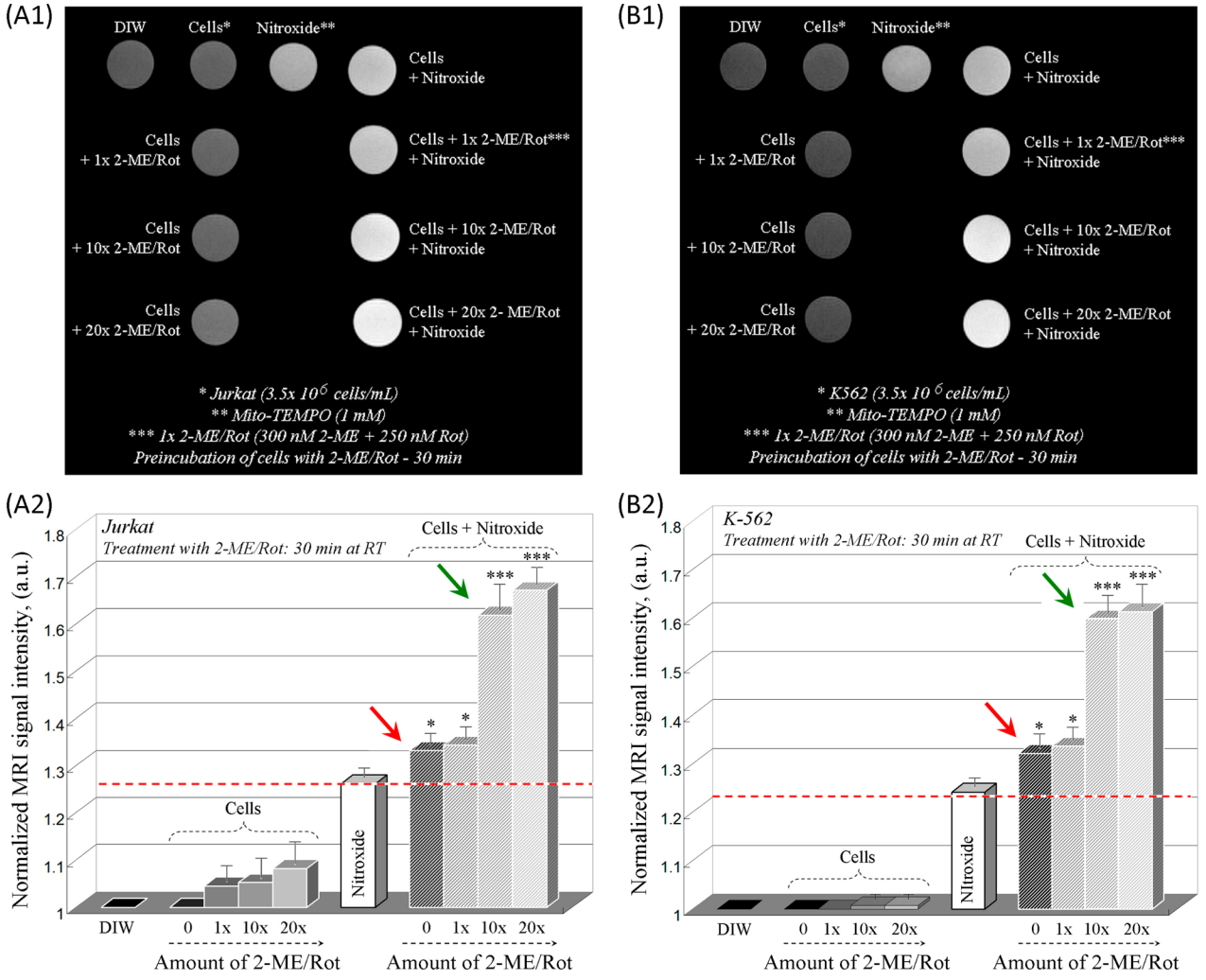

Figure 4. (A1, B1) Representative MR images of cell suspensions (A, Jurkat; B, K562) before and after incubation with 2-methoxyestradiol + rotenone (2-ME/Rot): "Acute treatment" protocol. Cells (3.5×10^6 cells/mL) were incubated for 30 min at room temperature (RT) with 1×, 10×, or 20× 2-ME/Rot (1× 2-ME/Rot = 300 nM 2-ME + 250 nM Rotenone). Untreated cells were used as a control. Each cell suspension was separated in two MRI phantoms (in equal volumes) and mito-TEMPO (1 mM) was added to one of them. All samples were subjected to T_1-weighted MRI (spin−echo) ∼20 min after addition of mito-TEMPO. Other controls: DIW, deionized water; Nitroxide, 1 mM mito-TEMPO in culture medium. (A2, B2) Normalized intensity of the MR signal of the phantoms, described in panels A1 and B1. Mean + SD values from six independent experiments are shown in the graphs: $*p < 0.05$; $**p < 0.01$; $***p < 0.001$ versus the MRI signal intensity of 1 mM mito-TEMPO in medium (the dotted red line).

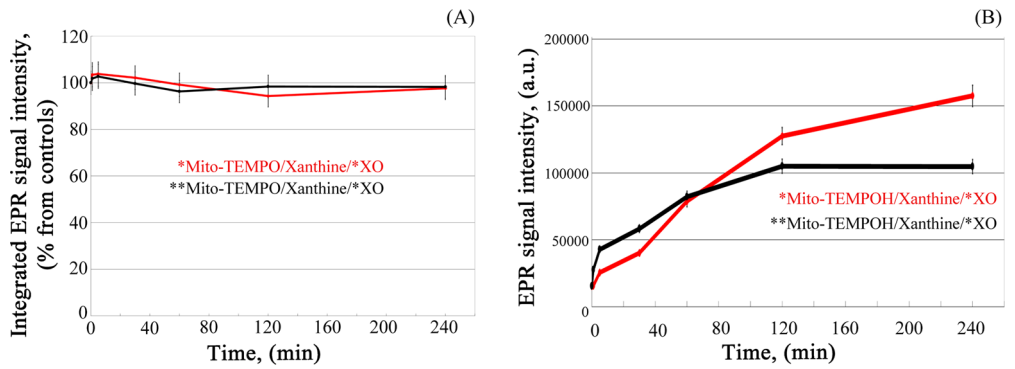

Figure 5. Dynamics of EPR signal intensity of mito-TEMPO (A) and mito-TEMPOH (B) in the presence of xanthine and xanthine oxidase: in black, 0.05 mM Mito-TEMPO (or mito-TEMPOH), 0.5 mM xanthine, and 0.05 U/mL xanthine oxidase; in red, 0.1 mM Mito-TEMPO (or mito-TEMPOH), 0.5 mM xanthine, 0.1 U/mL xanthine oxidase. Experimental conditions: The incubation was performed at room temperature, and EPR spectra were recorded at different time-intervals. Controls were mito-TEMPO or mito-TEMPOH (in the subsequent concentration), dissolved in buffer. Mean ± SD values from three independent experiments are shown in the figure.

DOI: 10.1021/acschemneuro.5b00220
ACS Chem. Neurosci. 2015, 6, 1922−1929

Information), as well as on cell suspensions. For example, the system xanthine/xanthine oxidase (which generates superoxide)[35] does not change the intensity of EPR signal of paramagnetic mito-TEMPO (Figure 5-A) but recovers the EPR signal of diamagnetic analogue mito-TEMPOH (Figure 5B). The EPR signal of mito-TEMPOH was also recovered by the system potassium superoxide/water (Figures 5S and 6S, Supporting Information). Hydrogen peroxide does not affect the intensity of EPR signal of both forms, paramagnetic and diamagnetic (Figure 7S, Supporting Information).

In conclusion, our study demonstrates a direct involvement of superoxide radical in the enhancement of T_1-weighted MRI signal in model systems and living cells in the absence and presence of nitroxide contrast probes. Nitroxide-enhanced T_1-weighted MRI (using mito-TEMPO as a contrast probe) allows visualization of overproduction of superoxide and is an appropriate technique for detection of mitochondrial dysfunction. This observation gives a direction for discovering of new opportunities for functional MRI, for example, detection of metabolic activity, which is accompanied by overproduction of superoxide (or other ROS, e.g., nitric oxide).

Our methodology allows visualization of the balance between superoxide and hydrogen peroxide in vitro and in vivo, which might be crucial for discovering the molecular nature of the cell signaling regulation and its disturbance in variety of pathologies (e.g., carcinogenesis, neurodegeneration, inflammation, autoimmune diseases, etc.). Moreover, the increased mitochondrial activity and the direct effect of the generated free radicals (e.g., superoxide, nitric oxide) and hydrogen peroxide on the proton relaxivity can give a direction for discovering of the molecular nature of the functional MRI in its commonly accepted definition, as a method for detection of the neurovascular coupling.

METHODS

Nitroxide Probes. Mito-TEMPO and mito-TEMPOH were purchased from Enzo Life Sciences. Deionized water (Milli-Q) was used in all experiments in model systems. The chemicals were analytical or HPLC grade.

Cells and Treatment Protocols. The cells (Jurkat and K562) were cultured in RPMI-1640 medium, supplemented with 10% fetal bovine serum and antibiotics (penicillin/streptomycin). Twenty-four hours before the experiment, the cells were replaced in a fresh medium without antibiotics. The mitochondrial function was impaired by incubation of cells with 2-methoxyestradiol (2-ME) and rotenone (Rot) at different concentrations and time intervals. Two experimental protocols were applied: (i) "mild treatment" and (ii) "acute treatment" of the cells by combination 2-ME/Rot.

Mild Treatment Protocol. The cells (200 μL of 3.5 × 10^6 cells/mL) were incubated with 300 nM 2-ME and 250 nM Rot (1× 2-ME/Rot) in 96-well plates for 24 h in humidified atmosphere (37 °C, 5% CO_2). In parallel, the same cells (200 μL of 3.5 × 10^6 cells/mL) were incubated with 5-fold higher concentrations of 2-ME/Rot, 1.5 μM 2-ME and 1.25 μM Rot (5× 2-ME/Rot) for 24 h, in humidified atmosphere.

Acute Treatment Protocol. The cells (200 μL of 3.5 × 10^6 cells/mL) were incubated with 3 μM 2-ME and 2.5 μM Rot (10× 2-ME/Rot) or 6 μM 2-ME and 5 μM Rot (20× 2-ME/Rot) for 30 min at room temperature (RT). In parallel, the same cells were incubated with 300 nM 2-ME and 250 nM Rot (1× 2-ME/Rot) for 30 min at RT.

After incubation, the cell suspensions were subjected to cell viability assay using trypan blue staining and automated counting of live/dead cells (Countess Automated Cell Counter, Invitrogen).

Dihydroethidium Assay of Superoxide. Dihydroethidium (DHE) is a cell-penetrating compound that, upon entering the cells, interacts with superoxide radicals and forms oxyethidium,[29] which in turn interacts with nucleic acids and emits a bright red color, which is detectable by fluorescent imaging devices (fluorescent microscopy, spectrofluorimetry, flow cytometry).[1,30] The major advantage of the DHE test is its ability to distinguish between superoxide and hydrogen peroxide.[31,32]

Briefly, DHE was dissolved in dimethyl sulfoxide (DMSO) to produce a 65 mM stock solution, which was diluted with PBS to prepare 6.5 μM DHA working solution on the day of experiment. The cell suspensions were adjusted to a concentration 1 × 10^6 cells/mL. DHA (10 μL) was added to 1 mL of each cell suspension. The samples were incubated for 60 min in the incubator (37 °C, 5% CO_2). They were collected by centrifugation at 1000 rpm for 10 min (at RT) and washed 3 times with phosphate-buffered saline solution (PBS; pH 7.4, with repetitive centrifugation). Finally, the cells were resuspended in 1 mL of PBS and placed in 96-well plates. The fluorescence intensity was detected using a microplate reader (TECAN Infinite M1000, Austria) at λ_{ex} = 518 nm and λ_{em} = 605 nm.

Magnetic Resonance Imaging. Two hundred microliters of each cell suspension was transferred to MRI phantoms. Ten microliters of mitochondria-penetrating nitroxide probe—mito-TEMPO (final concentration 1 mM) was added to the cell suspensions and incubated for 30 min at room temperature before the MRI measurement. Control samples contained (i) untreated cell suspensions without mito-TEMPO, (ii) 2-ME/Rot-treated cell suspensions without mito-TEMPO, and (iii) mito-TEMPO (1 mM) dissolved in culture medium.

MRI measurements were performed on a 7.0 T horizontal magnet (Kobelco and Jastec, Japan), interfaced with a Bruker Avance console (Bruker BioSpin, Germany) and controlled with the ParaVision 4.0.1 program (Bruker BioSpin, Germany). The phantoms were placed in the ^{1}H volume radio frequency (RF) resonator (Bruker BioSpin) with a surface RF receiver (RAPID Biomedical, Germany). The resonator units were placed in the magnet bore.

The MRI measurement was performed at the following parameters: T_1-weighted (spin-echo); repetition time = 250 ms; echo time = 9.6 ms; flip angle = 180°; field of view = 5.2 × 4.0 cm^2; number of averages = 4; slice thickness = 2 mm. The MRI data were analyzed using *ParaVision* software. All data were normalized to the sample with deionized water (DIW).

EPR Spectroscopy. Mito-TEMPO (or mito-TEMPOH) was dissolved in 100 mM PBS (pH 7.4) containing 25 μM diethylenetriaminepentaacetic acid (DTPA) as transition metal chelator (to avoid Fenton reactions). Two concentrations of mito-TEMPO (or mito-TEMPOH) were prepared, 0.05 and 0.1 mM. Xanthine (dissolved in the same buffer) was added to the mixture (final concentration 0.5 mM). The reaction was started by addition of xanthine oxidase (dissolved in the same buffer; final concentration 0.05 or 0.1 U/mL). This experimental protocol is recommended from Bruker for EPR detection of the superoxide free radicals with the nitrone spin traps in the xanthine/xanthine oxidase system.[35] Aliquots (100 μL) of each sample were placed in a glass capillary, and X-band EPR spectra were recorded on an X-band EPR instrument (Bruker) with a TE-mode cavity. All EPR measurements were performed under the following conditions: microwave frequency = 9.4 GHz; magnetic field strength = 336 mT; microwave power = 2.0 mW; field modulation frequency = 100 kHz; field modulation amplitude = 0.063 mT; time constant = 0.01 s; sweep width = 10 mT; scan time (sweep time) = 1 min. EPR spectra were recorded before addition of nitroxide and after addition of nitroxide (at various time intervals). EPR spectra were integrated. The data were presented in arbitrary units (au) or as a percentage from the respective control (nitroxide dissolved in PBS or culture medium).

ASSOCIATED CONTENT

Supporting Information

The Supporting Information is available free of charge on the ACS Publications website at DOI: 10.1021/acschemneuro.5b00220.

DOI: 10.1021/acschemneuro.5b00220
ACS Chem. Neurosci. 2015, 6, 1922−1929

Level of superoxide in Jurkat cells treated with 2-ME/Rot by conventional DHE test, effect of 2-ME/Rot on cell viability, Biochemical strategy to enhance superoxide accumulation in cells, effect of superoxide and hydrogen peroxide on the intensity of T_1-weighted MRI signal of deionized water, MRI signal intensity of TEMPOL (2 mM) and TEMPOL/ascorbate (1:1, mol/mol) in the presence of H_2O_2, $K_3Fe(CN)_6$, and KO_2, dynamics of EPR signal intensity of mito-TEMPOH (1 mM) in the absence and presence of KO_2, dynamics of EPR signal intensity of TEMPOL (1 mM) in the presence of ascorbate (1:1, mol/mol) with subsequent addition of KO_2 (2 mM) or H_2O_2, dynamics of EPR signal intensity of TEMPOL (1 mM) in the presence of H_2O_2 (PDF)

AUTHOR INFORMATION

Corresponding Author

*Rumiana Bakalova. Tel. +81-43-206-3872. E-mail: bakalova@nirs.go.jp.

Notes

The authors declare no competing financial interest.

ACKNOWLEDGMENTS

The participation of Mr. Masayuki Ozawa (Molecular Imaging Center, NIRS, Japan) in the MRI measurements is gratefully acknowledged. The study was partially supported by Grant-in-Aid "Kakenhi" from the Ministry of Education, Science and Technology of Japan.

REFERENCES

(1) Pelicano, H., Feng, L., Zhou, Y., Carew, J. S., Hileman, E. O., Plunkett, W., Keating, M. J., and Huang, P. (2003) Inhibition of mitochondrial respiration: A novel strategy to enhance drug-induced apoptosis in human leukemia cells by a reactive oxygen species-mediated mechanism. *J. Biol. Chem. 278*, 37832−37839.

(2) Saybasili, H., Yuksel, M., Haklar, G., and Yalcin, A. S. (2001) Effect of mitochondrial electron transport inhibitors on superoxide radical generation in rat hippocampal and striatal slices. *Antioxid. Redox Signaling 3*, 1099−1104.

(3) Staniek, K., Gille, L., Kozlov, A. V., and Nohl, H. (2002) Mitochondrial superoxide radical formation is controlled by electron bifurcation to the high and low potential pathways. *Free Radical Res. 36*, 381−387.

(4) Sabharwal, S. S., and Schumacker, P. T. (2014) Mitochondrial ROS in cancer: initiators, amplifiers or an Achilès heel? *Nat. Rev. Cancer 14*, 709−721.

(5) Hayashi, G., and Cortopassi, G. (2015) Oxidative stress in inherited mitochondrial diseases. *Free Radical Biol. Med.*, DOI: 10.1016/j.freeradbiomed.2015.05.039.

(6) Desideri, E., Vegliante, R., and Ciriolo, M. R. (2015) Mitochondrial dysfunction in cancer: genetic defects and oncogenic signalling impinging on TCA cycle activity. *Cancer Lett. 356*, 217−223.

(7) Tan, A. S., Baty, J. W., and Berridge, M. V. (2014) The role of mitochondrial electron transport in tumorogenesis and metastasis. *Biochim. Biophys. Acta, Gen. Subj. 1840*, 1454−1463.

(8) Yadav, A., Agarwal, S., Tiwari, S. K., and Chaturvedi, R. K. (2014) Mitochondria: prospective targets for neuroprotection in Parkinsoǹs disease. *Curr. Pharm. Des. 20*, 5558−5573.

(9) Pinto, M., and Moraes, C. T. (2014) Mitochondrial genome changes and neurodegenerative diseases. *Biochim. Biophys. Acta, Mol. Basis Dis. 1842*, 1198−1207.

(10) Trachootham, D., Alexandre, J., and Huang, P. (2009) Targeting cancer cells by ROS-mediated mechanisms: a radical therapeutic approach? *Nat. Rev. Drug Discovery 8*, 579−591.

(11) Fulda, S., Galluzzi, L., and Kroemer, G. (2010) Targeting mitochondria for cancer therapy. *Nat. Rev. Drug Discovery 9*, 447−464.

(12) Ivanova, D., Bakalova, R., Lazarova, D., Gadjeva, V., and Zhelev, Z. (2013) The impact of reactive oxygen species on anticancer therapeutic strategies. *Adv. Clin. Exp. Med. 22*, 899−908.

(13) Vila, M., and Przedborski, S. (2003) Targeting programmed cell death in neurodegenerative diseases. *Nat. Rev. Neurosci. 4*, 365−375.

(14) Jackson-Lewis, V., and Przedborski, S. (2007) Protocol for the MPTP mouse model of Parkinson's disease. *Nat. Protocols 2*, 141−151.

(15) Bakalova, R., Zhelev, Z., Aoki, I., and Saga, T. (2013) Tissue redox activity as a hallmark of carcinogenesis: from early to terminal stages of cancer. *Clin. Cancer Res. 19*, 2503−2517.

(16) Zhelev, Z., Aoki, I., Gadjeva, V., Nikolova, B., Bakalova, R., and Saga, T. (2013) Tissue redox activity as a sensing platform for imaging of cancer based on nitroxide redox cycle. *Eur. J. Cancer 49*, 1467−1478.

(17) Zhelev, Z., Bakalova, R., Aoki, I., Lazarova, D., and Saga, T. (2013) Imaging of superoxide generation in the dopaminergic area of the brain in Parkinson's disease, using mito-TEMPO. *ACS Chem. Neurosci. 4*, 1439−1445.

(18) Mehlhorn, R. J. (1991) Ascorbate- and dehydroascorbic acid-mediated reduction of free radicals in the human erythrocytes. *J. Biol. Chem. 266*, 2724−2731.

(19) Fuchs, J., Groth, N., Herrling, T., and Zimmer, G. (1997) Electron paramagnetic resonance studies on nitroxide radical 2,2,5,5-tetramethyl-4-piperidin-1-oxyl (TEMPO) redox reactions in human skin. *Free Radical Biol. Med. 22*, 967−976.

(20) Ui, I., Okajo, A., Endo, K., Utsumi, H., and Matsumoto, K. (2004) Effect of hydrogen peroxide in redox status estimation using nitroxyl spin probe. *Free Radical Biol. Med. 37*, 2012−2017.

(21) Bobko, A. A., Kirilyuk, I. A., Grigor'ev, I. A., Zweier, J. L., and Khramtsov, V. V. (2007) Reversible reduction of nitroxides to hydroxylamines: the roles for ascorbate and glutathione. *Free Radical Biol. Med. 42*, 404−412.

(22) Batinic-Haberle, I., Reboucas, J. S., and Spasijevic, I. (2010) Superoxide dismutase mimetics: chemistry, pharmacology, and therapeutic potential. *Antioxid. Redox Signaling 13*, 877−918.

(23) Davis, R. M., Matsumoto, S., Bernardo, M., Sowers, A., Matsumoto, K., Krishna, M. C., and Mitchell, J. (2011) Magnetic resonance imaging of organic contrast agents in mice: capturing the whole-body redox landscape. *Free Radical Biol. Med. 50*, 459−468.

(24) Huang, P., Feng, L., Oldham, E. A., Keating, M. J., and Plunkett, W. (2000) Superoxide dismutase as a target for the selective killing of cancer cells. *Nature 407*, 390−395.

(25) Kachadourian, R., Liochev, S. I., Cabelli, D. E., Patel, M. N., Frodovich, I., and Day, B. J. (2001) 2-Methoxyestradiol does not inhibit superoxide dismutase. *Arch. Biochem. Biophys. 392*, 349−353.

(26) Thews, O., Lambert, C., Kelleher, D. K., Biesalski, H. K., Vaupel, P., and Frank, J. (2005) Possible protective effects of alpha-tocopherol on enhanced induction of ROS by 2-methoxyestradiol in tumors. *Adv. Exp. Med. Biol. 566*, 349−355.

(27) Florczak, U., Toulany, M., Kehlbach, R., and Rodemann, H. P. (2009) 2-Methoxyestradiol-induced radiosensitization is independent of SOD, but depends on inhibition of Akt and DNA-PKcs activities. *Radiother. Oncol. 92*, 334−338.

(28) Ting, C. M., Lee, Y. M., Wong, C. K., Wong, A. S., Lung, H. L., Lung, M. L., Lo, K. W., Wong, R. N., and Mak, N. K. (2010) 2-Methoxyestradiol induces endoreduplication through the induction of mitochondrial oxidative stress and the activation of MAPK signalling pathways. *Biochem. Pharmacol. 79*, 825−841.

(29) Zhao, H., Kalivendi, S., Zhang, H., Joseph, J., Nithipatikom, K., Vasquez-Vivar, J., and Kalyanaraman, B. (2003) Superoxide reacts with hydroethidine but forms a fluorescent product that is distinctly different from ethidium: potential implications in intracellular fluorescence detection of superoxide. *Free Radical Biol. Med. 34*, 1359−1368.

(30) Tarpey, M. M., Wink, D. A., and Grisham, M. B. (2004) Methods for detection of reactive metabolites of oxygen and nitrogen: in vitro and in vivo considerations. *Am. J. Physiol. Regul. Integr. Comp. Physiol. 286*, R431−R444.

DOI: 10.1021/acschemneuro.5b00220
ACS Chem. Neurosci. 2015, 6, 1922−1929

(31) Fernandes, D. C., Wosniak, J., Pescatore, L. A., Bertoline, M. A., Liberman, M., Laurindo, F., and Santos, C. X. (2007) Analysis of dihydroethidium-derived oxidation products by HPLC in the assessment of superoxide production and NADPH oxidase activity in vascular systems. *Am. J. Physiol. Cell Physiol. 292*, C413−C422.
(32) Zielonka, J., Sarna, T., Roberts, J. E., Wishart, J. F., and Kalyanaraman, B. (2006) Pulse radiolysis and steady-state analyses of the reaction between hydroethidine and superoxide and other oxidants. *Arch. Biochem. Biophys. 456*, 39−47.
(33) Pervaiz, S., and Clement, M. V. (2007) Superoxide anion: Oncogenic reactive oxygen species? *Int. J. Biochem. Cell Biol. 39*, 1297−1304.
(34) Lurie, D. J. (2003) Proton-electron double-resonance imaging (PEDRI). *Biol. Magn. Reson. 18*, 547−578.
(35) Bruker website. (2015) EPR detection of the superoxide free radical with the nitrone spin traps DMPO and BMPO [https://www.bruker.com/fileadmin/user_upload/8-PDF-Docs/MagneticResonance/EPR_brochures/superoxide.pdf].

DOI: 10.1021/acschemneuro.5b00220
ACS Chem. Neurosci. 2015, 6, 1922−1929